

Preparation and Anticorrosive Properties of Oligoaniline Modified Silica Coatings

Yuwei Ye^{1,2}, Wei Liu¹, Zhiyong Liu¹, Haichao Zhao^{2*}, Liping Wang^{2*}

¹ Corrosion & Protection Centre, University of Science & Technology Beijing, Beijing 100083, China;

² Key Laboratory of Marine Materials and Related Technology, Zhejiang Key Laboratory of Marine Materials and Protective Technologies, Ningbo Institute of Materials Technology & Engineering, Chinese Academy of Sciences, Ningbo, 315201, China

*E-mail: zhaohaichao@nimte.ac.cn, wangliping@nimte.ac.cn

Received: 1 July 2017 / Accepted: 26 August 2017 / Published: 12 October 2017

Novel trianiline-containing sol-gel hybrid coatings were prepared by one-step electrodeposition technology on the surface of Q235 steel. The chemical component, microstructure of the as-prepared coatings were measured by FTIR, UV-vis, SEM. The effects of deposition time on the thickness, contact angle (CA) and surface roughness of coatings were investigated. The results showed that the modified silica coatings exhibited an excellent hydrophobic nature. By comparing with various deposition times (100, 300, 500, 700 s) under the deposition potential of -1.5 V, the coating under the deposition time of 500 s presented the best anti-corrosion effectiveness for bare steel substrate in 3.5 wt.% NaCl solution as verified by Tafel curves and electrochemical impedance spectroscopy (EIS).

Keywords: Oligoaniline; Sol-Gel coating; Electrodeposition; Corrosion resistance; Hydrophobicity

1. INTRODUCTION

Organic/inorganic hybrid coatings, combination of the advantages of organic and inorganic materials, have many potential applications including optical devices, catalysts, composites, and protective coatings with enhanced corrosion, scratch and wear-resistant performance [1-10]. For example, Wu et al. [11] successfully developed the silica hybrid materials on mild steel substrate via one-step electrodeposition technology and found that the silica hybrid materials presented a super hydrophobicity property. Zhang et al. [12] carefully acquired the silica hybrid materials by electrodeposition process and indicated that the as-deposited silica hybrid materials owed an excellent

anti-corrosion performance in 3.5 wt.% NaCl solution. Peng et al. [13] prepared the organic-inorganic hybrid silica coating on copper surface by sol-gel method and discovered that combining the silica coating and benzotriazole (BTA) could obviously enhance the corrosion protection property of copper. Peng et al. [14] also connected the epoxy modified sol-gel silica material and thiourea (TUA) to form a novel organic-inorganic hybrid coating and hinted that the corrosion resistance of silica + TUA coating was better than that of pure sol-gel silica coating. However, after prolonged immersion in corrosive medium, the corrosion protection properties of hybrid silica coating presented obviously downtrend, which could not reach the demand in some extreme environments [15, 16].

Incorporation of functional building blocks to the organic-inorganic hybrid network has been widely studied for improving the anticorrosion performance of coating material [17-19]. Polyaniline (PANi) as a kind of conducting polymer is widely used in some organic coatings owing to its ease of synthesis, inexpensiveness and special redox behavior [20-23]. However, few studies have been reported on the application of PANi in the organic/inorganic hybrid protective coatings [24, 25]. Meanwhile, some reports pointed out that the main challenges in applying PANi for anticorrosion fields are due to its weak solubility and less functionality [26, 27]. In contrast, oligoanilines exhibit much improved solubility in organic solvent and possess end functional group, while maintaining similar electrical properties to those of PANi [28-31]. Several oligoaniline containing anticorrosive polymers have been developed including aniline trimer containing epoxy [32], polyimide [33], polyurea [34] and photocurable methacrylate coatings [35]. Tetraaniline based hybrid anticorrosive coatings was also successfully developed by sol-gel reaction of organosilane capped tetraaniline and triethoxymethylsilane (TEMS) [26].

Thus, the purpose of this study was to prepare a novel oligoaniline-containing silica hybrid coating by electrodeposition technology and discussed the relationships between deposition time and anti-corrosion performances of oligoaniline-containing silica hybrid coatings on low-carbon steel in 3.5 wt.% NaCl solution. Meanwhile, the anticorrosion mechanism of coating was emphatically researched, which could provide a certain degree of scientific guiding value for its practical application in corrosion environment.

2. EXPERIMENTAL SECTION

2.1. Materials

Triethoxysilylpropyl isocyanate (TESPIC), anhydrous tetrahydrofuran (THF), n-hexane and tetraethoxysilane (TEOS) were purchased from Aladdin Industrial Corporation. N, N'-diaminodiphenylamine, ammonium persulfate, ammonium hydroxide, acetone, ethanol, sodium nitrate, hydrochloric acid and acetic acid were purchased from Sinopharm Chemical Reagent Co. Ltd. Most of chemicals and solvents were used as received without further purification. The Q235 mild steel specimens (10 mm × 10 mm × 10 mm, with composition of 1.39 wt.% C, 0.29 wt.% Mn, 0.18 wt.% Al and balanced Fe (wt.%) were polished using 400, 800 and 1500-grit sand papers. After that, for purpose of removing the surface impurities and preventing the electrode rust, the Q235 steel electrodes

were rinsed by ultrasonication in acetone and ethyl alcohol, and finally dry in nitrogen. The aniline trimer (AT) and N, N'-Bis(4'-(3-triethoxysilylpropylureido)-phenyl)-1,4-quinonediimine (TSUPQD) were produced according to the reported document [28].

2.2 Preparation of trianiline modified silica coating by electrodeposition

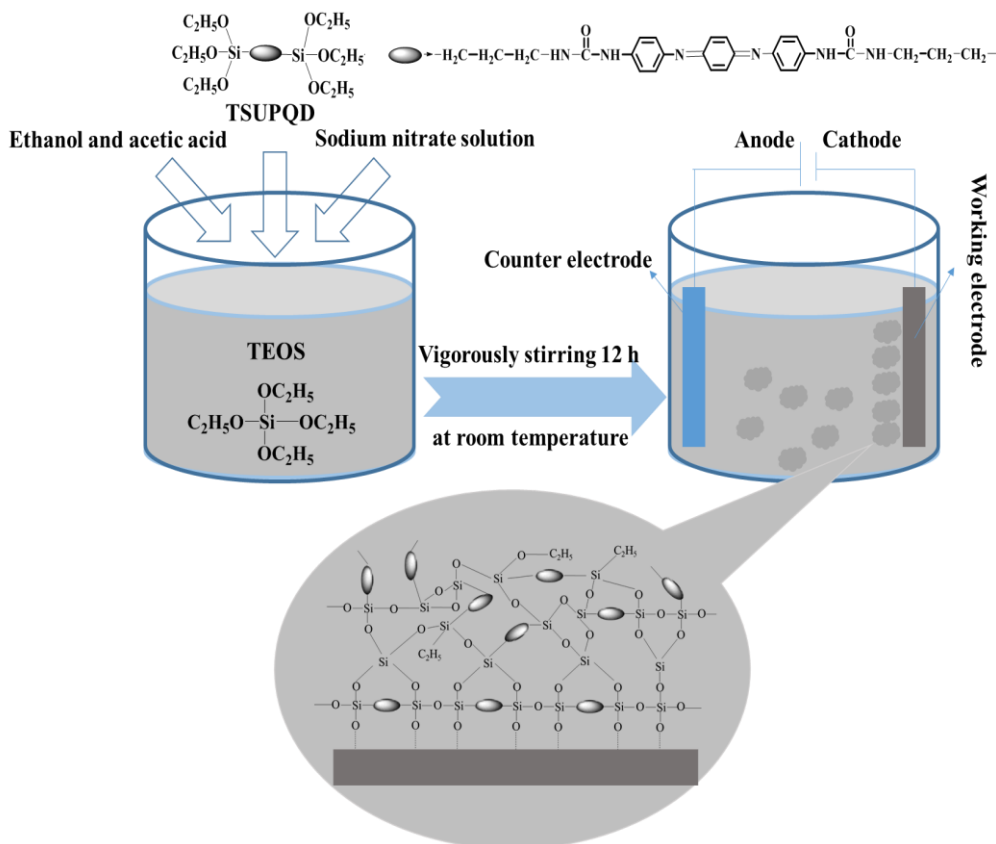


Figure 1. The schematic illustration for preparation of oligoaniline-containing silica coating.

A novel modified silica coating was successfully acquired by electrodeposition method and the schematic diagram was shown in Fig.1. Specifically, TEOS (2 g), TSUPQD (0.04 g), ethanol (80 ml), sodium nitrate solution (20 ml, 0.01 mol/L) and acetic acid (adjust PH at 4.5) were mixed in a beaker with vigorous stirring for 12 h. Prior to mixing, the as-prepared TSUPQD was dissolved in ethanol and sonicated for 30 min. After hydrolysis, the mixed solution was used as a precursor solution, the electrodeposition process was built on a CHI-660E workstation (Chenhua, Shanghai) with a three-electrode system, which contained the work electrode (Q235 steel), the counter electrode (platinum plate) and the reference electrode (saturated potassium chloride). The deposition potential was -1.5 V and the deposition times were 100, 300, 500, 700 s. For convenience, the coatings with different deposition times (100, 300, 500, 700 s) were marked as T-100, T-300, T-500, T-700 coatings, respectively. After that, these samples were rinsed with ethanol and deionized water, and then dried in a vacuum oven for 5 h at 40 °C.

2.3 Characterization

The chemical compositions and organizations of as-prepared coatings were characterized by NICOLET 6700 transform infrared spectroscopy (FTIR), the wavenumber of FTIR was ranged from 500 to 3500 cm^{-1} and the wavelength of UV-vis spectrum was recorded from 250 to 800 nm. The FEI Quanta FEG 250 Field Emission Scanning Electron Microscope (FE-SEM) was used to analyze the surface morphologies of these coatings. Electron gun acceleration voltage of electron gun was set to 8 ~ 10 kV and selected the ETD detector for imaging analysis. The CA was measured by an OCA20 contact angle analyzer with water according to the sessile drop method.

2.4 Electrochemical measurements

The CHI-660E workstation (Chenhua, Shanghai) was used to characterize the potentiodynamic polarization measurements and electrochemical impedance spectroscopy of these coatings in 3.5 wt.% NaCl solution. At the temperature of 20 ± 5 °C, the mild steel (10 mm \times 10 mm), the platinum plate (2.5 cm^2), and the saturated potassium chloride were selected as the working electrode, counter electrode and the reference electrode, respectively. The corrosion potential (E_{corr}) and corrosion current density (i_{corr}) were obtained by the measurement of Tafel curves. The electrochemical impedance spectroscopy was collected at a frequency of 10^5 to 10^{-2} Hz with using amplitude of 15 mV AC signal. The potentiodynamic polarization measurements were obtained from cathodic direction to anodic direction ($E_{\text{ocp}} \pm 250$ mV) with the rate of 0.2 mV/s. The inhibition efficiency of IE% was calculated from corrosion current density (i_{corr}) using the following equation 1 [31]:

$$IE\% = \frac{i_{\text{corr}}^0 - i_{\text{corr}}}{i_{\text{corr}}^0} \times 100\% \quad (1)$$

where i_{corr}^0 and i_{corr} signified the corrosion current density uncoated and coated Q235 steel, respectively. In addition, in order to analysis the corrosion situation, the corrosion morphologies of coatings were recorded by the FEI Quanta FEG 250 SEM.

3. RESULTS AND DISCUSSION

3.1 Characterization of the hybrid coatings

Fig.2 showed the FTIR spectrum of T-500 coating. Clearly, a broad peak in the region of 1000~1200 cm^{-1} were found, which assigned to the stretching vibration of Si-OH and Si-O-Si network. Meanwhile, some new absorption peaks such as 1672, 1510, 1588, 1314 and 1165 cm^{-1} were observed on the modified silica coating, corresponding to the carbonyl groups, the benzenoid (B) ring stretching vibrations, the quinonoid (Q) ring stretching vibrations, the C-N stretching of aromatic amines and the -N=Q=N- stretching vibrations, respectively [36-38].

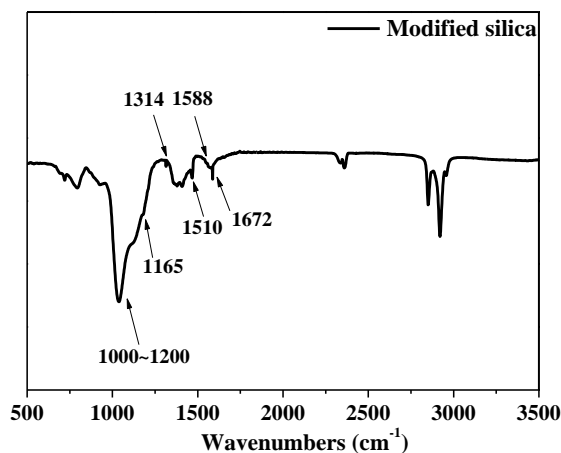


Figure 2. FTIR spectrum of T-500 coating

The UV-vis spectrum of T-500 coating was displayed in Fig.3. It is obviously that two absorption peaks were seen in the UV-vis region for the modified silica coating, which centered at 312 and 553 nm, corresponding to the π - π^* transition of the conjugated ring system and the benzenoid-to-quinoid excitonic transition, respectively [39-41], which was due to the existence of aniline trimers in modified silica coating.

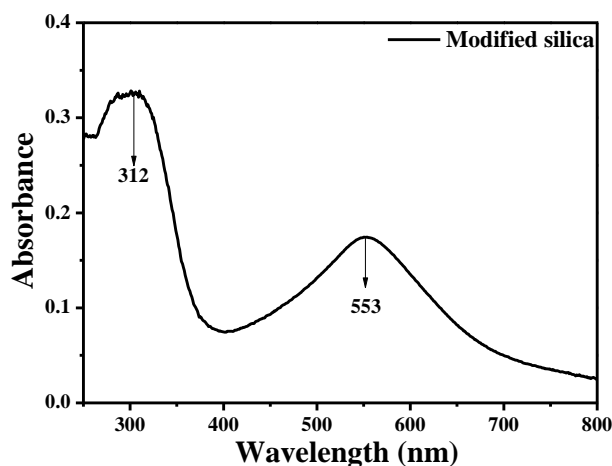


Figure 3. UV-vis spectrum of T-500 coating

The surface morphologies and CA of modified silica coatings were shown in Fig.4. The surface of bare substrate was smooth and the CA was about 52.8°, indicating an obvious hydrophilic nature (Fig.4a). For modified silica coating, at the deposition condition of 100 s, the coating revealed a hierarchical morphology and some silica particles were observed on the surface, the CA was about 137.9°, indicating an obvious hydrophobic nature (Fig.4b). When the deposition time increased to 300 and 500 s, the amount of silica particle was obviously increased, the CA were sharply enhanced to 153.5° and 154.7°, respectively, implying a significantly super hydrophobic property (Fig.4c and d). When the deposition time further increased, it could be seen that the CA and surface coverage showed decreasing trend (Fig.4e).

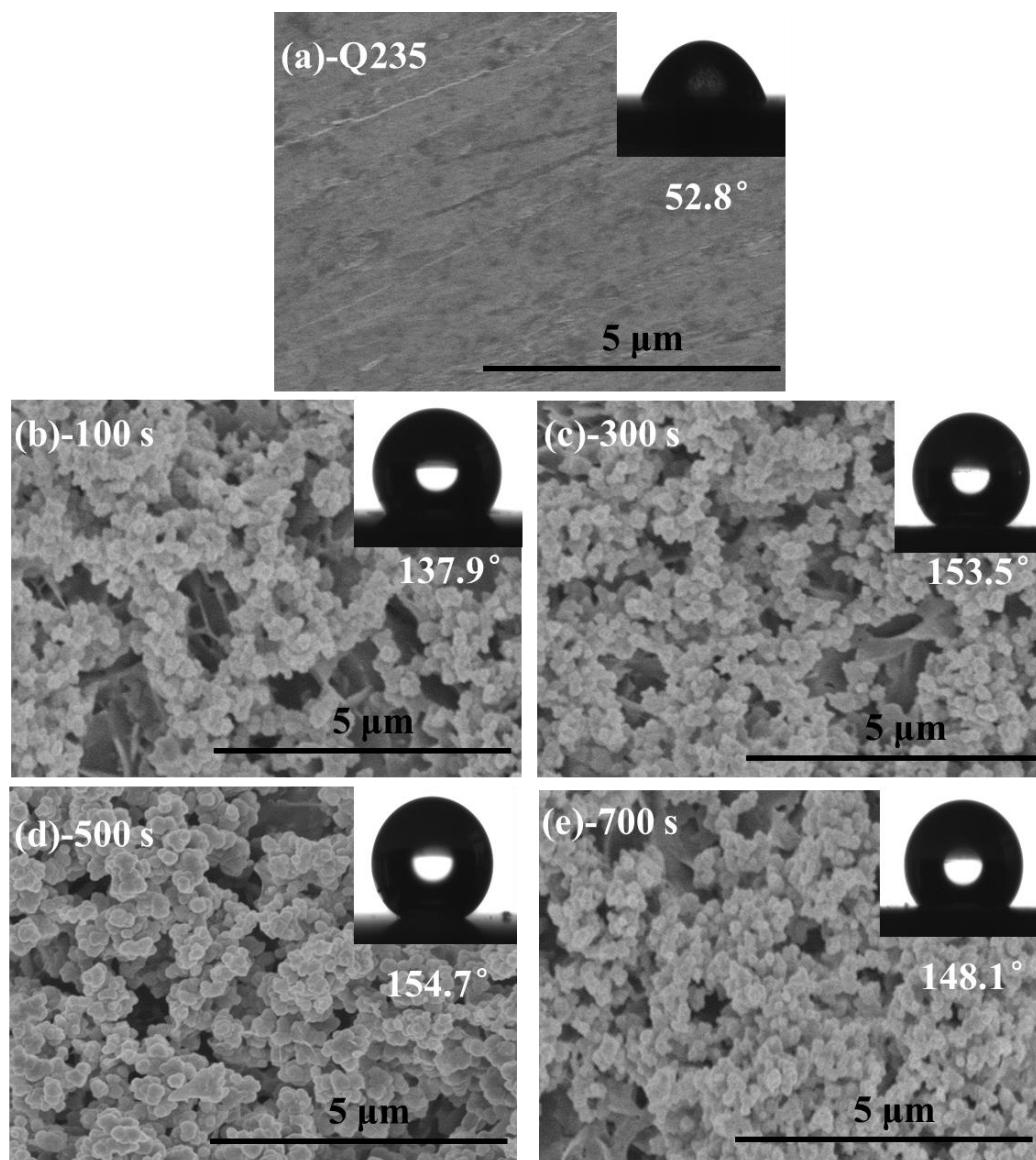


Figure 4. The surface morphologies and CA values of these modified silica coatings in different deposition times (a) Q235 (b) 100 s (c) 300 s (d) 500 s (e) 700 s

In order to explore the detail relationships between the surface roughness, thickness and deposition time, the results were listed in Fig.5. Significantly, the surface roughness (Ra) and deposition rate (thickness) of modified silica coating increased sharply with the deposition time ranging from 100 to 500 s, this was due to more quantity of OH^- catalysts were produced, which could accelerate the formation of coating [12]. After this critical point (500 s) was exceeded, the surface roughness and coating thickness began to decrease, which was probably due to the agglomeration of silica particles under long times [12].

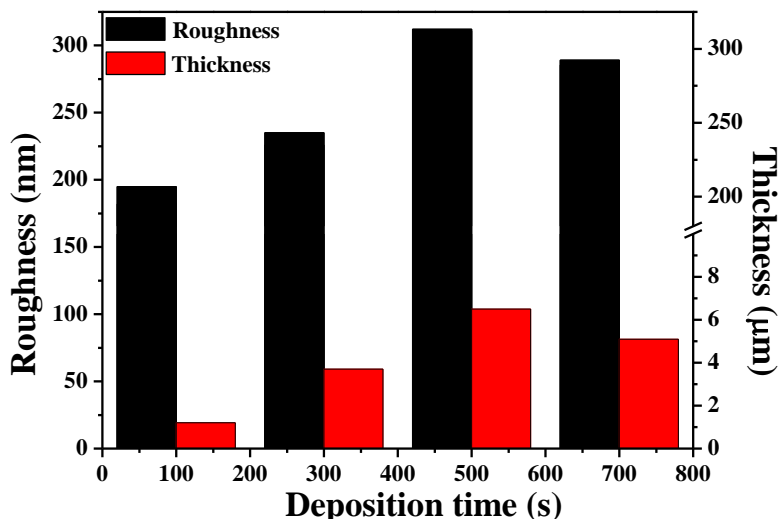


Figure 5. The relationships between the surface roughness, thickness and deposition time of these modified silica coatings

3.2 Polarization curves

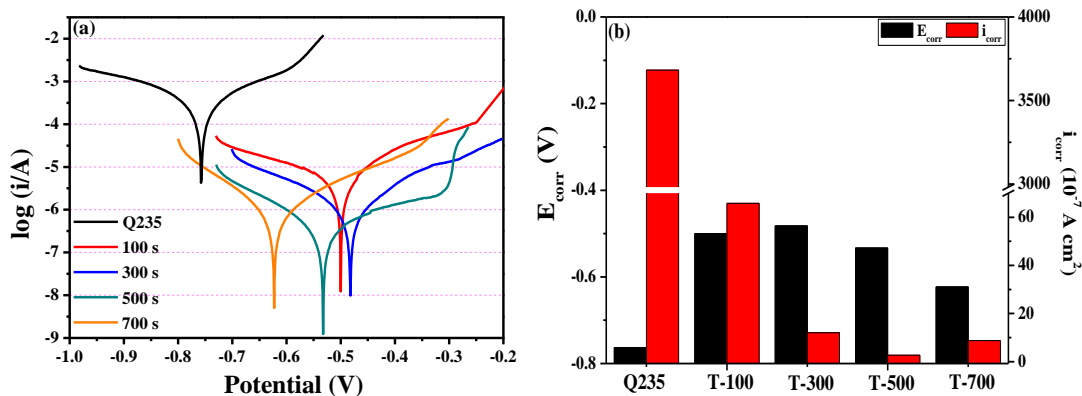


Figure 6. Tafel curves, E_{corr} and i_{corr} of these modified silica coatings at different deposition times

After soaked in 3.5 wt.% NaCl solution for 168 h, the Tafel curves, E_{corr} and i_{corr} of bare substrate and these modified silica coatings were summarized in Fig.6. Obviously, compared to bare substrate, it could be seen that the corrosion potential of coating shifted to the positive direction (Fig.6a), manifesting that the coating acted as a barrier isolation to prevent the intrusion of corrosion medium [42]. Meanwhile, the corrosion current densities (i_{corr}) of these modified coatings were 2~3 orders of magnitude lower than that of bare steel, indicating the greatly enhancement of corrosion resistance. The improvement mechanism was attributed to the generation of passive film on the surface of steel, which caused by the special redox catalytic abilities of aniline trimer units in modified silica coatings [43]. The i_{corr} of T-500 coating reached to the lowest value of $2.7 \times 10^{-7} A cm^2$ (Fig.6b), which was 96.4%, 77.5% and 69.4% lower than T-100, T-300 and T-700 coatings, respectively, implying the

best anti-corrosion property. The polarization resistance of R_p was calculated by Stearn–Geary equation [44]:

$$R_p = \frac{b_a b_c}{2.303(b_a + b_c) i_{corr}} \quad (2)$$

Here, b_a is anodic Tafel slope and b_c is cathodic Tafel slope. These values and IE% were listed in Table 1. It is clearly that the value of b_a revealed an increasing and then decreasing trend, hinting that aniline trimer in T-500 coating could effectively restrain the anodic reaction [45]. In addition, the R_p of T-500 coating was 21.8, 4.9 and 4.1 times than that of T-100, T-300 and T-700 coatings, respectively, and the IE% was 98.21%, 99.67%, 99.93% and 99.76% for T-100, T-300, T-500 and T-700 coatings, respectively, indicating the T-500 coating owning more electroactive portion presented better inhibition efficiency [46].

Table 1. Anodic Tafel slopes (b_a), cathodic Tafel slopes (b_c), R_p and IE of all coatings

Samples	b_a mV dec ⁻¹	b_c mV dec ⁻¹	R_p Ω cm ²	IE %
100 s	69.71	40.09	6213.1	98.21
300 s	85.84	59.58	27831.7	99.67
500 s	199.28	55.69	135734.3	99.93
700 s	102.92	191.56	33462.4	99.76

3.3 Electrochemical impedance spectroscopy (EIS)

Fig.7 displayed the electrochemical impedance spectroscopy (EIS) of modified silica coatings in 3.5 wt.% NaCl solution. In generally, the $|Z|_{0.01 \text{ Hz}}$ and $\phi_{10^5 \text{ Hz}}$ are used to measure the ability of coating to prevent corrosion. The higher the $|Z|_{0.01 \text{ Hz}}$ and $\phi_{10^5 \text{ Hz}}$ are, the stronger the corrosion resistance is. At the condition of 100 s, the $|Z|_{0.01 \text{ Hz}}$ and $\phi_{10^5 \text{ Hz}}$ were about $6.5 \times 10^5 \text{ Ω cm}^2$ and 39.8° after 24 h soaking, respectively (Fig. 7a and e). With the increase of soaking time, the $|Z|_{0.01 \text{ Hz}}$ and $\phi_{10^5 \text{ Hz}}$ presented descending trend, implying that the anticorrosion property of T-100 coating showed a decline trend with the permeation of corrosion solution [47]. With the increase of deposition time, the $|Z|_{0.01 \text{ Hz}}$ and $\phi_{10^5 \text{ Hz}}$ showed rising trend until 500 s, where reached the max values of $3.5 \times 10^6 \text{ Ω cm}^2$ and 45.1° (Fig. 7c and g). This might due to the super hydrophobic surface and the highest coating thickness of T-500 coating. The super hydrophobic surface could vastly avoid the adsorption of water and then decreased the permeation of corrosion medium [1]. The hybrid coating with a large thickness could provide a complex infiltration route for corrosion solution and then the penetration time to reach the bare substrate was delayed [48]. When the deposition time further increased, the $|Z|_{0.01 \text{ Hz}}$ and $\phi_{10^5 \text{ Hz}}$ descended slightly (Fig. 7d and h).

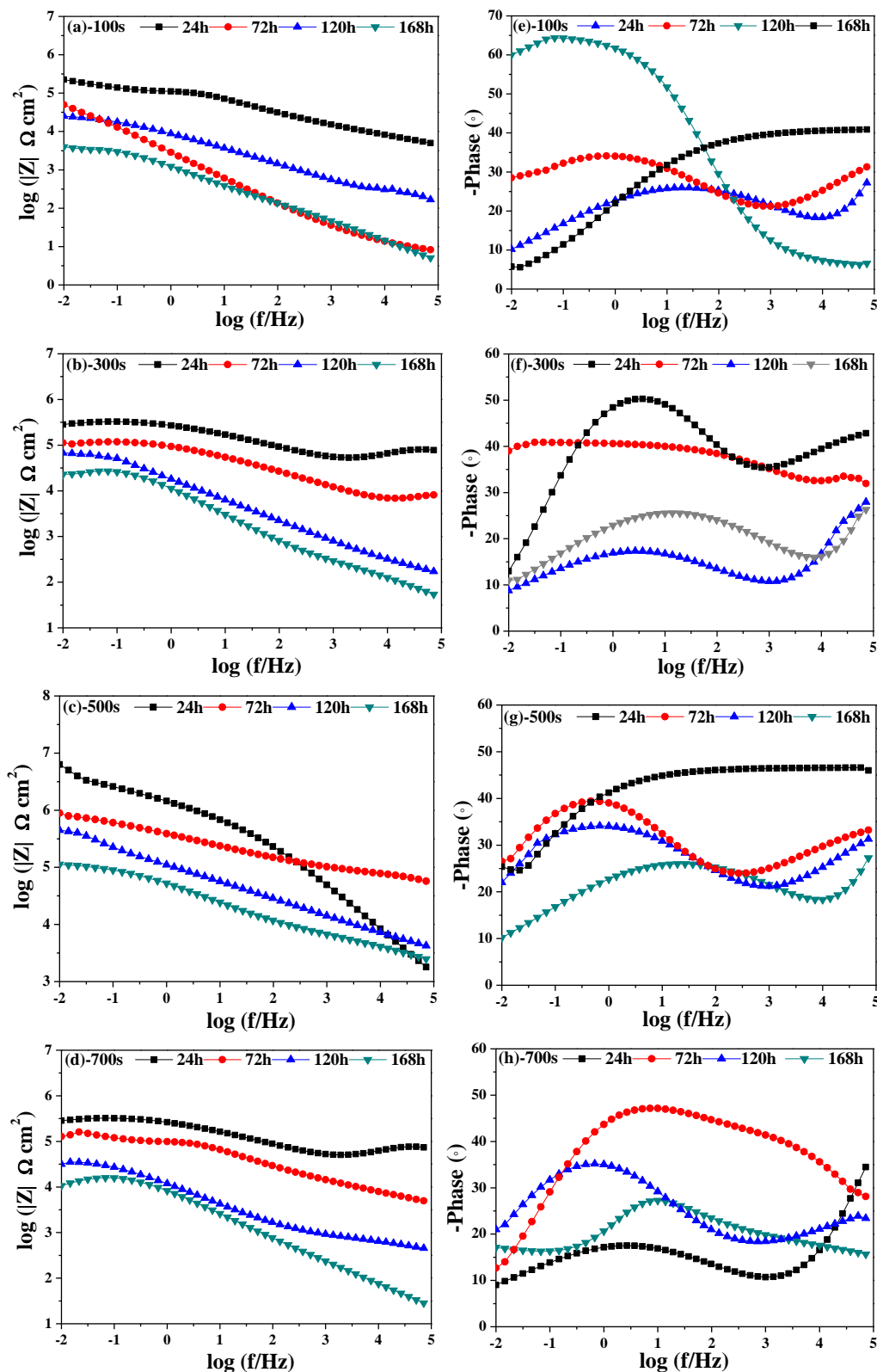


Figure 7. The electrochemical impedance spectroscopy (EIS) of these modified silica coatings in 3.5 wt.% NaCl solution (a)(e) 100 s (b)(f) 300 s (c)(g) 500 s (d)(h) 700 s

The equivalent electrical circuit of these coatings was shown in Fig. 8. Among them, R_s , R_c and R_{ct} represented the solution resistance, pore resistance of the coating and the charge-transfer resistance,

respectively. C_c and C_{dl} represented the coating capacitance and double-layer capacitance, respectively. By measurement, the R_c , R_{ct} , C_c and C_{dl} of all coatings in different soaking times were shown in Fig.9. For T-100 coating, the R_c and R_{ct} were about 226 and 83.7 $K\Omega\ cm^2$ after 24 h soaking, respectively. When the soaking time increased to 168 h, the R_c and R_{ct} decreased to 32 and 2.22 $K\Omega\ cm^2$, respectively, which were reduced by 85.8% and 97.3%, respectively (Fig.9a and b), indicating the degradation of coating [49].

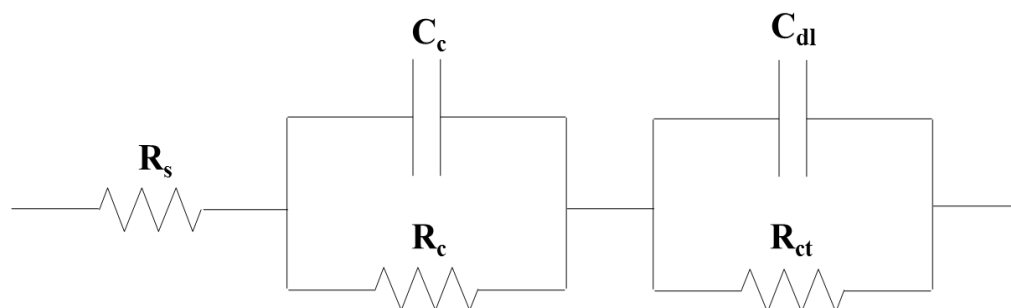


Figure 8. The equivalent electrical circuit of these modified silica coatings

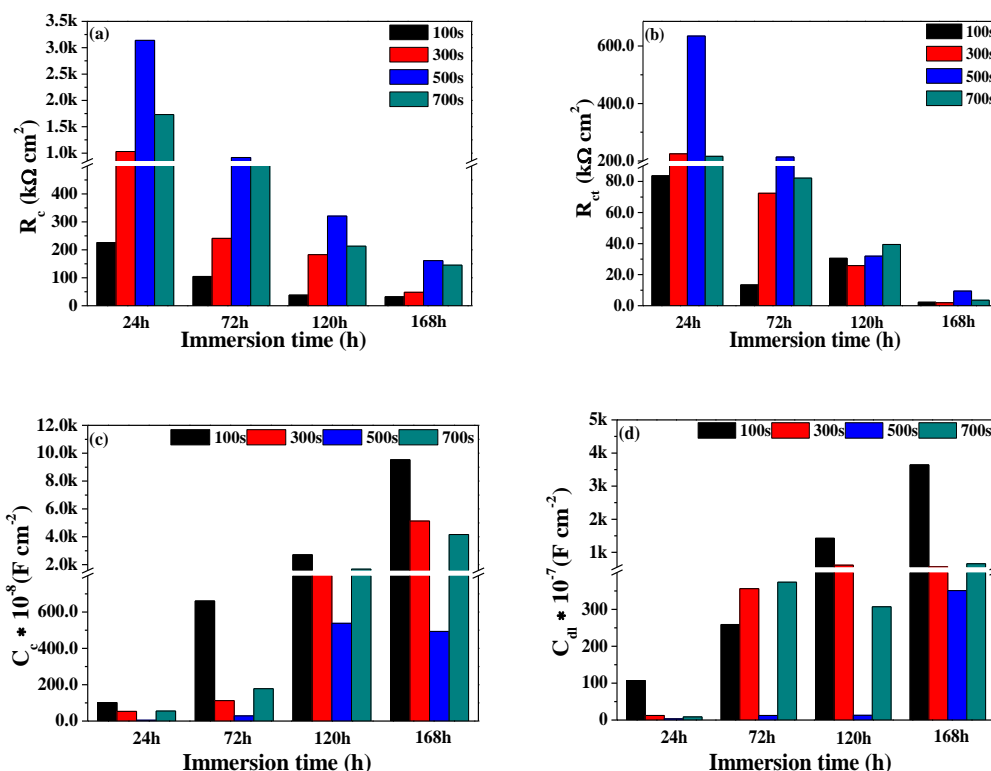


Figure 9. The R_c , R_{ct} , C_c and C_{dl} of these modified silica coatings with different deposition times in different soaking times (a) R_c , (b) R_{ct} , (c) C_c and (d) C_{dl}

With the increase of deposition time, the R_c and R_{ct} showed increasing trend until 500 s, where the R_c and R_{ct} achieved the max values. The enhancement of R_c and R_{ct} were imputed to the generation of passive film by the special redox catalytic abilities of aniline trimer units on the surface of steel, which reinforced the protective function of coating and reduced the electrotransfer between bare steel

and corrosion medium [44, 50]. Nevertheless, the R_c and R_{ct} showed downtrend when the deposition time further increased. Different to R_c and R_{ct} , the C_c and C_{dl} presented opposite rule. The change of C_c was because of the invasion of oxygen and water, which increased the local dielectric constant of coating [51]. The augment of C_{dl} was ascribed to the variation of corrosion area of electrode in the test [26, 52].

3.4 Contact angle in different immersion times

Coating with a superhydrophobic surface could serve as valid physical barriers during the corrosion test [53]. Fig.10 showed the CA values of these modified silica coatings with different immersion times in 3.5 wt.% NaCl solution. After soaked in 3.5 wt.% NaCl solution for 24 h, the CA of T-100 coating was about 133.9°. When the soaking time increased to 168 h, the CA decreased to 119.8°. The decline of CA was attributed to the erosion of Cl^- ions, which owned a forceful destructive effect on passivation film and the surface structure of coating [54]. As the deposition time increased, the CA presented an obviously enhancement and reached the highest value at the deposition time of 500 s. After soaking for 168 h, the CA of T-500 coating was still up to about 144.8°, indicating a good hydrophobic nature. Because of this, the erosion effect of chloride ion was the weakest on the surface of T-500 coating [55].

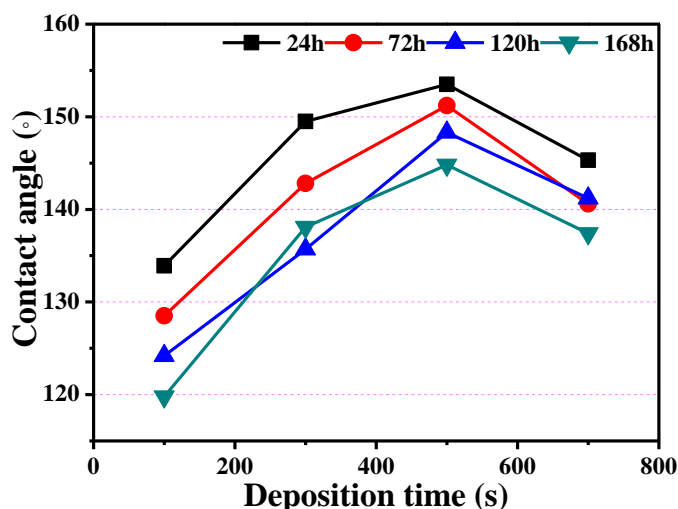


Figure 10. CA values of these modified silica coatings with different immersion times in 3.5 wt.% NaCl solution

3.5 Corrosion Morphologies

After soaked in 3.5 wt.% NaCl solution, the corrosion morphologies of these modified silica coatings with different deposition times were shown in Fig. 11. It was observed that some cracks and corrosion chippings on the surface of T-100 and T-300 coatings (Fig. 11a and b). However, when the

deposition time increased to 500 s, the surface was relatively smooth and flat, no obvious cracks and corrosion chippings were found on the surface of T-500 coating (Fig. 11c). When the deposition time increased to 700 s, some slightly cracks and holes were distributed on the surface of T-700 coating, indicating a slight decrease of corrosion resistance (Fig. 11d). In summary, the deposition time was an important parameter to affect the anti-corrosion properties of the coatings, and the modified silica coating at the deposition time of 500 s exhibited the best corrosion resistance in 3.5 wt.% NaCl solution.

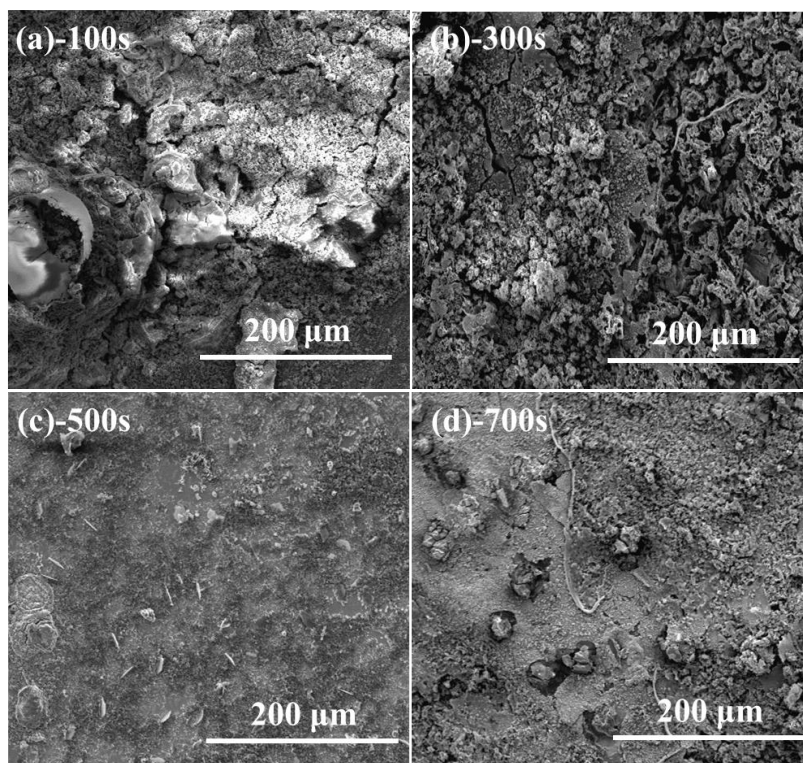


Figure 11. Corrosion morphologies of these modified silica coatings with different deposition times (a) 100 s (b) 300 s (c) 500 s (d) 700 s

4. CONCLUSIONS

In this study, novel aniline trimer modified silica coatings were successfully fabricated by one-step electrochemical deposition for the corrosion protection of Q235 steel. The surface roughness, coating thickness and CA of hybrid coatings could be well-controlled by adjusting the deposition time during the deposition process. Meanwhile, the deposition time was an important factor to change the corrosion resistance of coating. With the increase of deposition time in the lower range (100~500 s) under the electro-potential of -1.5 V, the corrosion current density of coating showed a descending trend and the electrochemical impedance of coating showed an ascending trend. However, opposite trends were observed when the deposition time further increased. As a result, the modified silica

coating deposited at the condition of 500 s showed the best anti-corrosion performance in corrosion medium of 3.5 wt.% NaCl solution.

ACKNOWLEDGEMENTS

The authors gratefully appreciate financial support provided by the National Basic Research Program of China (973 Program project, No. 2014CB643300); the Strategic Priority Research Program of the Chinese Academy of Sciences (XDA13040601); “One Hundred Talented People” of the Chinese Academy of Sciences [No. Y60707WR04]; Natural Science Foundation of Zhejiang Province [No. Y16B040008].

References

1. D. Zhang, H. Qian, L. Wang, X. Li, *Corro. Sci.*, 103 (2016) 230-241.
2. H. Qian, D. Xu, C. Du, D. Zhang, X. Li, L. Huang, L. Deng, Y. Tu, J. M. C. Molc, H. A. Terryn, *J. Mater. Chem. A.*, 5 (2017) 2355-2364.
3. D. Zhang, L. Wang, H. Qian, X. Li, *J. Coat. Technol. Res.*, 13 (2016) 11-29.
4. K. Wasiński, P. Nowicki, P. Pórolniczak, M. Walkowiak, R. Pietrzak, *Int. J. Electrochem. Sci.*, 12 (2017) 128-143.
5. Y. Lai, C. Lin, H. Wang, J. Huang, H. Zhuang, L. Sun, *Electrochem. Commun.*, 10 (2008) 387–391.
6. A. S. Fouda, M. A. Diab, S. Fathy, *Int. J. Electrochem. Sci.*, 12 (2017) 347-362.
7. M. L. Ma, R. M. Hill, J. L. Lowery, S.V. Fridrikh, G. C. Rutledge, *Langmuir*, 21 (2005) 5549–5554.
8. X. Wang, H. Xiao, *Int. J. Electrochem. Sci.*, 12 (2017) 268-279.
9. G. A. El-Mahdy, A. M. Atta, H. A. Al-Lohedan, A. M. Tawfik, A. A. Abdel-Khalek, *Int. J. Electrochem. Sci.*, 10 (2015) 151-161.
10. L. Zhai, F.C. Cebeci, R.E. Cohen, M.F. Rubner, *Nano. Letters.*, 4 (2004) 1349–1353.
11. L. K. Wu, J. M. Hu, J. Q. Zhang, *J. Mater. Chem. A.*, 1 (2013) 14471-14475.
12. X. F. Zhang, R. J. Chen, J. M. Hu, *Corro. Sci.*, 104 (2016) 336-343.
13. S. Peng, Z. Zeng, W. Zhao, H. Li, Q. Xue, X. Wu, *Surf. Coat. Technol.*, 213 (2012) 175–192.
14. S. Peng, W. Zhao, H. Li, Z. Zeng, Q. Xue, X. Wu, *Appl. Surf. Sci.*, 276 (2013) 284–290.
15. F. Zucchi, V. Grassi, A. Frignani, G. Trabaneli, *Corros. Sci.*, 46 (2004) 2853–2865.
16. F. Zucchi, A. Frignani, V. Grassi, G. Trabaneli, M. DalColle, *Corros. Sci.*, 49 (2007) 1570–1583.
17. C. Sanchez, B. Lebeau, F. Chaput and J. P. Boilot, *Adv. Mater.*, 15 (2003) 1969–1994.
18. A. Walcarius, *Chem. Mater.*, 13 (2001) 3351–3372.
19. D. Wang, G. P. Bierwagen, *Prog. Org. Coat.*, 64 (2009) 327–338.
20. J. Jang, J. Ha, S. Kim, *Macromol. Res.*, 15 (2007) 154–159.
21. Y. Chen, X. H. Wang, J. Li, J. L. Lu, F. S. Wang, *Electrochim. Acta.*, 52 (2007) 5392–5399.
22. Y. P. Li, H. M. Zhang, X. H. Wang, J. Li, F. S. Wang, *Corros. Sci.*, 53 (2011) 4044–4049.
23. T. I. Yang, C. W. Peng, Y. L. Lin, C. J. Weng, G. Edgington, A. Mylonakis, T. C. Huang, C. H. Hsu, J. M. Yeh, Y. Wei, *J. Mater. Chem.*, 22 (2012) 15845–15852.
24. H. Wang, R. Akid, M. Gobara, *Corro. Sci.*, 52 (2010) 2565–2570.
25. R. Akid, M. Gobara, H. Wang, *Electrochim. Acta.*, 56 (2011) 2483–2492.
26. L. Gu, S. Liu, H. Zhao, H. Yu, *RSC. Adv.*, 5 (2015) 56011-56019.
27. J.Q. Dong, *J. Appl. Polym. Sci.*, 126 (2012) 10-16.
28. Y. Guo, A. Mylonakis, Z. Zhang, P. I. Lelkes, K. Levon, S. Li, Q. Feng, Y. Wei, *Macromolecules*, 40 (2007) 2721-2729.
29. S. C. Lin, C. S. Wu, J. M. Yeh, Y. L. Liu, *Polym. Chem.*, 5 (2014) 4235-4244.

30. K. C. Chang, H. I. Lu, C. W. Peng, M. C. Lai, S. C. Hsu, M. H. Hsu, Y. K. Tsai, C. H. Chang, W. I. Hung, Y. Wei, J. M. Yeh, *ACS Appl. Mater. Interfaces.*, 5 (2013) 1460–1467.
31. C. J. Weng, C. H. Chang, C. W. Peng, S.W. Chen, J. M. Yeh, C. L. Hsu, Y. Wei, *Chem. Mater.*, 23 (2011) 2075–2083.
32. K. Huang, C. Shiu, P. Wu, Y. Wei, J. Yeh, W. Li, *Electrochim. Acta.*, 54 (2009) 5400–5407.
33. Y. Yu, J. Yeh, S. Liou, Y. Chang, *Acta. Mater.*, 52 (2004) 475–486.
34. P. D. Tatiya, R. K. Hedao, P. P. Mahulikar, V. V. Gite, *Ind. Eng. Chem. Res.*, 52 (2013) 1562–1570.
35. S. Mohamadpour, B. Pourabbas, P. Fabbri, *Sci. Iran. F.*, 18 (2011) 765–771.
36. S. Quillard, G. Louarn, S. Lefrant, A.G. Macdiarmid, *Phys. Rev. B. Condens. Matter.*, 50 (1994) 12496–12508.
37. I. Harada, Y. Furukawa, F. Ueda, *Synth. Met.*, 29 (1989) 303–312.
38. Y. Furukawa, F. Ueda, Y. Hyodo, I. Harada, T. Nakajima, T. Kawagoe, *Macromolecules*, 21 (1988) 1297–1305.
39. H. Wang, P. Guo, Y. Han, *Macromol. Rapid Commun.*, 27 (2006) 63–68.
40. Z. Yang, X. Wang, Y. Yang, Y. Liao, Y. Wei, X. Xie, *Langmuir*, 26 (2010) 9386–9392.
41. L. Chen, Y. Yu, H. Mao, X. Lu, W. Zhang, Y. Wei, *Mater. Lett.*, 59 (2005) 2446–2450.
42. A. P. Hanza, R. Naderi, E. Kowsari, M. Sayebani, *Corros. Sci.*, 107 (2016) 96–106.
43. H. Huang, T. Huang, T. Yeh, C. Tsai, C. Lai, M. Tsai, J. Yeh, Y. Chou, *Polymer*, 52 (2011) 2391–2400.
44. J.M. Yeh, C.F. Hsieh, J.H. Jaw, T.H. Kuo, H.Y. Huang, C.L. Lin, M.Y. Hsu, *J. Appl. Polym. Sci.*, 95 (2005) 1082–1090.
45. K. R. Ansari, M. A. Quraishi, A. Singh, *Corros. Sci.*, 79 (2014) 5–15.
46. K. Huang, C. Shiu, P. Wu, Y. Wei, J. Yeh, W. Li, *Electrochim. Acta.*, 54 (2009) 5400–5407.
47. S. Qiu, C. Chen, W. Zheng, W. Li, H. Zhao, L. Wang, *Synth. Met.*, 229 (2017) 39–46.
48. M. Shokouhfar, C. Dehghanian, M. Montazeri, A. Baradaran, *Appl. Surf. Sci.*, 258 (2012) 2416–2423.
49. F. Mansfeld, *Electrochim. Acta.*, 35 (1990) 1533–1544.
50. S. S. Abd El Rehim, S. M. Sayyah, M. M. El-Deeb, S. M. Kamal, R. E. Azooz, *Int. J. Ind. chem.*, 7 (2016) 39–52.
51. A. Kosari, M.H. Moayed, A. Davoodi, R. Parvizi, M. Momeni, H. Eshghi, H. Moradi, *Corros. Sci.*, 78 (2014) 138–150.
52. H. Huang, X. Guo, G. Zhang, Z. Dong, *Corros. Sci.*, 53 (2011) 3446–3449.
53. X. Zhang, R. Chen, Y. Liu, J. Hu, *J. Mater. Chem. A.*, 4 (2016) 649–656.
54. L. Shan, Y. Wang, J. Li, J. Chen, *Surf. Coat. Technol.*, 242 (2014) 74–82.
55. C. Chen, S. Qiu, S. Qin, G. Yan, H. Zhao, L. Wang, *Int. J. Electrochem. Sci.*, 12 (2017) 3417–3431.